Micropore Size Distributions of Activated Carbons and Carbon Molecular Sieves Assessed by High-Pressure Methane and Carbon Dioxide Adsorption Isotherms

D. Lozano-Castelló, D. Cazorla-Amorós,* A. Linares-Solano, and D. F. Quinn†

Departamento de Química Inorgánica, Universidad de Alicante, E-03080, Alicante, Spain

Received: February 27, 2002; In Final Form: July 3, 2002

Experimental N_2 adsorption isotherms and high-pressure CO_2 and CH_4 adsorption isotherms have been obtained for a series of microporous carbon materials prepared for being used in gas separation and methane storage. The shape of the isotherms is very different, which is due in part to differences in the overall micropore volume but, additionally and importantly, to the significant differences in the micropore size distribution of those samples. Micropore size distributions (MPSDs) have been deduced from those N_2, CO_2, and CH_4 isotherms by application of the General Adsorption Isotherm (GAI), according to two different approaches proposed in previous independent works. The comparison of the results has shown that, despite the different characteristics of CH_4 and CO_2, and the different experimental temperatures and adsorption conditions (298 K, supercritical conditions, and 273 K, subcritical conditions, respectively), a quite good consistency between the MPSDs from these two gases has been obtained for all the samples studied. That suggests that both methods are suitable to analyze more sensibly the changes in the MPSDs of microporous samples. The fact that these MPSDs analysis are based on high-pressure adsorption isotherms and that CO_2 is especially useful for characterizing the narrow microporosity not accessible to N_2 makes both techniques very useful for the characterization of microporous samples.

1. Introduction

Carbonaceous adsorbents are widely used in many different processes. Among others, two interesting applications on which we are focused are natural gas storage and gas separation. Storage of natural gas with carbon materials at low pressures (e.g., 4 MPa) has been considered a promising technology for use in natural-gas fueled vehicles.[1−3] Moreover, it is also being considered for applications such as end of pipeline storage, peak shaving, or even for bulk transportation of natural gas. On the other hand, the use of carbon molecular sieves (CMS) in gas separations (O_2/N_2, CO_2/CH_4, etc.) has been constantly growing.

The carbon materials required for these applications must be designed and prepared in such a way that the porous texture is the most suitable for each application. Several studies have been carried out in our laboratory to prepare carbon materials, which present the best performance in those two applications.[4−9] When the carbon materials are produced, the characterization of their porous texture is crucial. Due to the considerable sensitivity of nitrogen adsorption isotherms to the pore structure in both the microporous and mesoporous regimes and to its relative experimental simplicity, measurements of subcritical nitrogen adsorption at 77 K are, undoubtedly, the most used to provide experimental input for characterization methods.

In the case of methane storage applications, linear relationships between the methane adsorption capacity at 298 K and microporosity obtained from 77 K N_2 adsorption measurements have been shown for many carbon adsorbents.[1,2,4] However, in a previous work,[9] it has been demonstrated that the methane adsorption capacity not only depends on the micropore volume but also strongly depends on the micropore size distribution. Those results are directly related to the theoretical[10−13] and experimental[14] studies, which showed that the methane density is very sensitive to the pore size width and that the maximum adsorptive methane density can be achieved in pores, with an effective pore width a bit less than 0.8 nm (in the present paper the pore width does not include the carbon atom forming the pore). Therefore, it is desirable to obtain a micropore size distribution, MPSD, for the proper assessment of carbons with a view to maximizing Adsorbed Natural Gas (ANG) storage.

In the case of gas separation applications, where nonequilibrium conditions exist, the micropore structure of carbon molecular sieves must be unique, since the slitlike apertures or the so-called "constrictions" of their micropores must be of a size similar to the molecular dimensions of the adsorbing species. In the separation of gases, molecules smaller than the size of the micropore constrictions would rapidly diffuse through them into the associated micropore volume, while a larger molecule would be denied access to the volume behind the constrictions within the time constraints used for the separation process.[15]

Thus, characterization by pore size distribution is indispensable for the utilization and design of improved porous carbons in those and many other applications.

As previously commented, N_2 at 77 K is the most widely used gas for the characterization of porous solids, and usually, has the special status of recommended adsorptive.[16] Thus, different methods to derive the micropore size distribution function were and are being developed mostly for this adsorptive: TVFM Methods,[17,18] Horvath−Kawazoe (HK) Method,[19] and simulation methods based on statistical mechanics.[20,21] However, the main disadvantage of N_2 adsorption at 77 K is that when it is used for the characterization of microporous solids, diffusional problems of the molecules inside the narrow

* Corresponding author. Fax: (34) 965 903454. E-mail: cazorla@ua.es.
† Current address: Department of Chemistry and Chemical Engineering, Royal Military College of Canada, P.O. Box 17000 STN FORCES, Kingston, ON K7K 7B4, Canada

10.1021/jp0205564 CCC: $22.00
Published on Web 08/16/2002

porosity range (size < 0.7 nm) occur.[22] Moreover, there is an additional experimental difficulty in the adsorption of subcritical nitrogen because very low relative pressures (10^{-8} to 10^{-4}) are required to extend the range of porosity studied to narrow microporosity. To overcome these problems, the use of other adsorptives has been proposed. In previous studies it has been shown that a good alternative to complement N_2 adsorption could be the use of CO_2 adsorption at 273 K[23−25] or CH_4 at 298 K.[26,27] Though the critical dimension of the CO_2 molecule is similar to that of N_2, the higher temperature of adsorption used for CO_2 results in a larger kinetic energy enabling the molecules to enter into the narrow porosity. However, the high vapor pressure of carbon dioxide at 273 K requires the use of high-pressure adsorption apparatus in order to cover the same range of relative pressure than in the case of N_2 at 77 K. Supercritical CH_4 at 298 K has a somewhat higher kinetic energy than CO_2 at 273 K so it can also penetrate into small pores that may not be available to nitrogen at 77 K.

Another reason for looking for other adsorbates and/or thermodynamic conditions for the characterization of porous solids include the need to mimic the conditions of the specific application. For example, it is useful to use supercritical methane adsorption to characterize an adsorbent proposed for the methane storage applications.[1,4,7,9,25,26,28]

The fact that adsorption of supercritical gases occurs mainly in micropore range sized pores make high-pressure adsorption a useful technique in the determination of micropore size distributions (MPSD), as it has been pointed out by Sosin and Quinn.[26] In that work[26] it was shown that when relatively high-pressure methane isotherms at room temperature were measured on carbons, differences in the overall uptake were very obvious. These differences are due in part to differences in the overall micropore volume, but additionally and importantly are due to differences in the MPSD of these carbons. In that work a method of determining micropore size distribution, MPSD, of carbon adsorbents based on the high-pressure methane isotherm was presented. This method requires relatively few isotherm points, fifteen or less, in a single isotherm, at a very convenient temperature. It is based on a generalized adsorption isotherm, GAI, which uses Monte Carlo simulation to obtain the local isotherm and so takes into account the variation in adsorbate density with changing pore width. It has been demonstrated that it is capable of identifying pore sizes and determining their pore volume for pores not detected by 77 K nitrogen.[27]

In addition to the use of supercritical methane adsorption, the adsorption of CO_2 up to pressures of 3 MPa has also been studied previously.[23−25] It was shown that high-pressure CO_2 adsorption at 273 K can be used to characterize the whole range of porosity (down to a pore size close to 0.4 nm). CO_2 adsorption at subatmospheric pressures is especially important to complement N_2 adsorption at 77 K since it is sensitive to the narrow micropores not accessible to N_2. Due to the wider range of relative fugacities (to about 0.7), in which adsorption in micropores occurs, this avoids the use of very low relative pressures as with N_2 at 77 K. Moreover, MPSDs have been deduced by application of the generalized adsorption isotherm (GAI) using the Dubinin-Radushkevich (DR) equation as the local adsorption isotherm.[24,25]

Thus, in those works,[23−26] it was shown that the use of high-pressure methods (CO_2 at 273 K and CH_4 at 298 K) for characterizing the MPSD of carbon materials was interesting. In fact, nowadays, applicability of high-pressure adsorption techniques and the fundamental study of adsorption by both gases on microporous materials is gaining attention. Recently, several models have been developed for the interfacial characterization of a microporous solid from high-pressure methane adsorption and for the prediction of high-pressure methane adsorption.[29−36] The development of models for the study of the adsorption of CO_2 at 273 K and subatmospheric pressures[37−39] and high pressure[35,36,39−41] have been also the objective of several studies.

Because of the importance of the characterization of microporous materials and the potential of high-pressure adsorption, the main objective of this work is to characterize in terms of micropore size distribution some of the carbon materials prepared in our laboratory for methane storage and gas separation applications. These materials have been prepared starting from the same raw material but depending on the preparation conditions they present different micropore volumes and very different MPSDs. All of the samples have been studied by N_2 (77 K) and CO_2 (273 K) at subatmospheric pressure and by high-pressure CO_2 adsorption at 273 K and CH_4 at 298 K. The MPSDs for all the materials have been deduced from N_2 and CO_2 adsorption according to previous work[24] and from the high-pressure methane isotherms.[26] In this paper, comparison of the porous texture (micropore volume and MPSDs) assessed by these three different adsorptives at low and high pressure is presented. It should be mentioned that, except for the work of Quirke et al.,[36] in which a comparison between CO_2 and CH_4 adsorption at pressures lower than 2 MPa has been done, and the recent work of Stoeckli et al.,[41] comparisons between the high-pressure adsorption of these two adsorptives have not been done previously.

2. Theory

N_2, CO_2, and CH_4 adsorption isotherms have been used to obtain information about micropore size distribution (MPSD) using the general adsorption isotherm (GAI)[42]

$$n(p) = \int_0^{\infty} v(L,p) f(L)\, \mathrm{d}L \tag{1}$$

where $n(p)$ is the experimental isotherm, $v(L,p)$ is the local adsorption isotherm, and $f(L)$ is the unknown pore size distribution. The approach developed by Sosin and Quinn[25] has been used for high-pressure methane isotherms. In that work $v(L,p)$ was derived using the results of Tan and Gubbins, who calculated the adsorbate densities using GCMC for the pressure range 0−6 MPa, for pore sizes ranging from 0.38 to 50 nm.[43] To obtain the MPSDs the method developed by Cazorla-Amoros et al.[24] has been used. The local isotherm employed for N_2 and CO_2 has been the DR equation.[44]

$$V/V_o = \exp(-1/(E_o\beta)^2 (RT \ln(p_o/p))^2) \tag{2}$$

DR equation applies well to adsorption systems involving only van der Waals forces and is especially useful to describe adsorption on activated carbon.[45] The main advantage of the DR theory is that it can be applied whatever the adsorbate and the temperature. To relate the characteristic energy and the pore size the following equation[46] has been used:

$$L(nm) = 10.8/(E_o - 11.4) \tag{3}$$

when the characteristic energy is between 42 and 20 kJ/mol. In that equation, L is the mean pore width, and E_o is the characteristic energy (kJ/mol). This range of energies corresponds to pore sizes between 0.35 and 1.3 nm for which the validity of this equation has been tested.[46] The Dubinin

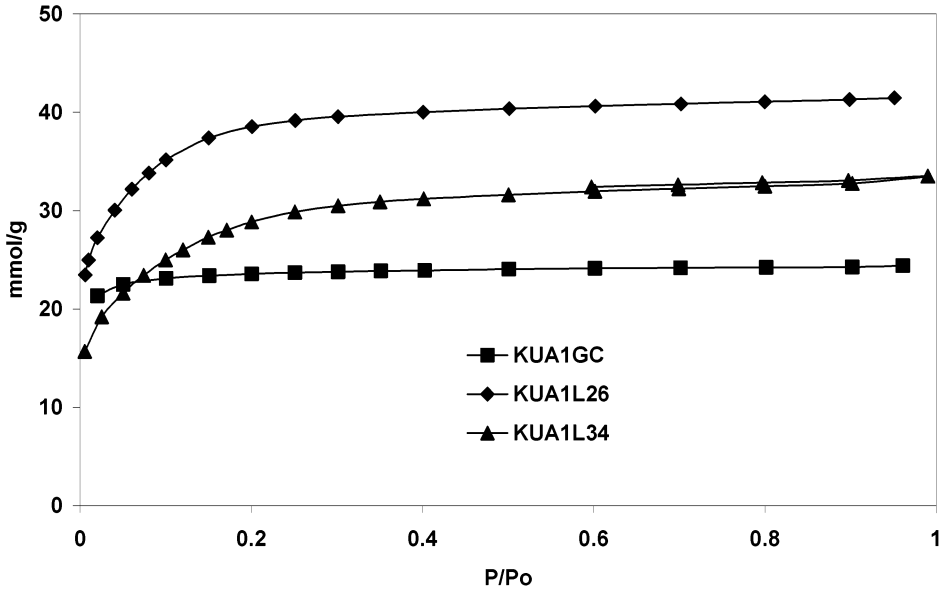

Figure 1. N_2 adsorption isotherms at 77 K corresponding to the three activated carbons.

equation[47] has been used for lower values of E_o (i.e., higher pore sizes).

$$L(nm) = 24/E_o \quad (4)$$

3. Experimental Section

Four carbon materials with different micropore structures have been selected for this study: (i) a carbon molecular sieve (KUA1B8) prepared in our laboratory by blocking the microporosity of a previously prepared activated carbon; and (ii) three activated carbons prepared by chemical activation with KOH of a Spanish anthracite (KUA1GC, KUA1L26 and KUA1L34). It should be mentioned that these samples are not just ordinary granulated activated carbons. They have been prepared as a result of an intensive study into the effect of the preparation variables on the final porosity of the activated carbon.[6] Thus, the samples have been chosen in such a way that their micropore volume and their MPSDs are very different due to the different activation conditions used. These specific porous textures, together with the fact that all the samples have been prepared from the same raw material, make them suitable for analyzing the applicability of the different methods for calculating the MPSD.

Porous texture analysis of all the samples has been carried out by subatmospheric N_2 and CO_2 adsorption at 77 K and 273 K, respectively, in an Autosorb 6 apparatus. CO_2 and CH_4 adsorption isotherms at 273 K and 298 K, respectively, and at high pressures have been obtained in a Sartorius high-pressure microbalance. The balance is equipped with a pressure indicator and a thermocouple mounted in the sample housing as well as with a rotary pump. The maximum pressure used in this study was 3 and 4 MPa for CO_2 and CH_4, respectively. The experimental results have been corrected for buoyancy effects[47] related to the displacement of gas by the sample, sample holder, adsorbed phase, and pan. The corrections due to the sample holder and pan were obtained with a blank experiment carried out with the sample holder empty. The buoyancy due to the sample, which results in an apparent loss of weight, was estimated as the product of the skeletal volume of the sample and gas density.[48] The buoyancy effect related to the adsorbed phase was corrected to obtain the absolute adsorption isotherms.[49] The high-pressure adsorption isotherms are reproducible to about 1% within the error of the balance.

TABLE 1: Porous Texture Characterization Results Obtained from N_2 (77 K) and CO_2 (273 K) Adsorption Data

sample	BET surface area (m^2/g)	$V(N_2)$ (cm^3/g)	$V(CO_2)$ (cm^3/g)
KUA1B8			0.20
KUA1GC	2021	0.83	0.80
KUA1L26	3290	1.45	0.81
KUA1L34	2402	1.07	0.52

4. Results and Discussion

4.1. N_2 (77 K) and CO_2 (273 K) Adsorption at Subatmospheric Pressure. Figure 1 shows the N_2 adsorption isotherms at 77 K of the three activated carbons. The N_2 adsorption isotherm corresponding to the carbon molecular sieve (KUA1B8) is not shown because this sample presents a very narrow microporosity, not accessible to N_2 at 77 K.[23,24] The kinetics of N_2 adsorption is extremely slow at 77 K, and extremely long times are necessary to reach the equilibrium at each point of the isotherm. However, in this narrow porosity CO_2 adsorption occurs more readily.[22−25] N_2 adsorption isotherms obtained for the activated carbons are of type I according to the IUPAC classification,[50] typical of essentially microporous samples.

Table 1 contains the micropore volumes obtained by applying the Dubinin-Radushkevich equation to the N_2 and CO_2 adsorption isotherms at 77 K and 273 K, respectively. The volume of narrow microporosity (pore size smaller than 0.7 nm) has been assessed from CO_2 adsorption at 273 K and subatmospheric pressures (V_{CO_2}).[22−24] From N_2 adsorption, the total micropore volume (V_{N_2}) (pore size lower than 2 nm) has been calculated. The densities used for liquid N_2 at 77 K and adsorbed CO_2 at 273 K have been, respectively, 0.808 and 1.023 g/mL, and the affinity coefficients used have been 0.33 and 0.35, for N_2 and CO_2, respectively. [22−24]

Table 1 shows that all the samples, except for the carbon molecular sieve, present a V_{N_2} higher than the V_{CO_2}. The difference between both micropore volumes (V_{N_2} and V_{CO_2}) in the case of the sample KUA1GC is very low, indicating that this sample presents a very homogeneous porosity, as can be also seen from the sharp knee of the N_2 adsorption isotherms.

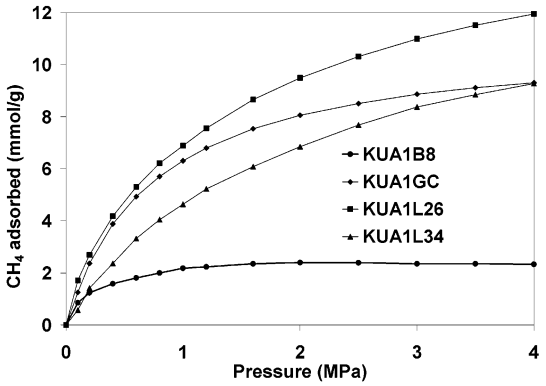

Figure 2. CH_4 adsorption isotherms at 298 K for all the samples studied. Points: experimental isotherms; lines: Toth equation curve fittings.

TABLE 2: Micropore Volume Calculated from High-Pressure CO_2 (273 K) and CH_4 (298 K) Adsorption Isotherms

sample	V (CO_2HP) (cm^3/g)	V (CH_4) (cm^3/g)
KUA1B8	0.18	0.24
KUA1GC	0.84	0.94
KUA1L26	1.22	1.17
KUA1L34	0.82	0.94

The sample KUA1L34 has the widest micropore size distribution and contains a significant proportion of supermicroporosity (0.7 < pore size < 2 nm), estimated as $V_{N_2} - V_{CO_2}$.[47] This is also reflected in the knee of the isotherm, which is rounder than in the case of the previous sample. The contrary occurs in the CMS ($V_{CO_2} > V_{N_2}$). It indicates the existence of narrow microporosity, where N_2 adsorption at 77 K has diffusional limitations.[22−25]

These characterization results clearly show that the samples chosen for this study have significant differences in pore size distribution. In addition, as previously commented, all of the samples have been prepared from the same raw material and the same type of activation process so that the structural differences are mainly due to the different micropore volumes and micropore size distributions. Thus, these samples are very suitable for studying the characterization by CO_2 and CH_4 high-pressure adsorption.

4.2. High-Pressure CH_4 (298 K) and CO_2 (273 K) Adsorption Isotherms. Figure 2 presents the experimental CH_4 adsorption isotherms at 298 K of all the samples studied shown as points. These isotherms have been smoothed by curve fitting using the Toth equation[53]

$$n(p) = \frac{mp}{(b + p^t)^{1/t}} \tag{5}$$

where $n(p)$ is the mass of methane adsorbed per unit mass of carbon at pressure p, and m, b, and t are parameters. Toth equation curve fittings are illustrated in Figure 2 as lines.

Figure 2 shows that the highest methane adsorption capacity at 4 MPa corresponds to the sample with the highest micropore volume (KUA1L26) (see Table 1). It can be seen that the methane adsorption capacity at 4 MPa for the samples KUA1GC and KUA1L34 is very similar. The micropore volumes determined from N_2 at 77 K or low-pressure 273 K CO_2 (see Table 1) for each of these carbons are quite different. However, analysis of the high-pressure 273 K CO_2 and the 298 K CH_4 isotherms concludes that both these carbons have very similar micropore volumes, (see Table 2) even though there is some difference in the overall values from these two gases. The difference in the shape of the methane isotherms in Figure 2 for these carbons relates to a difference in pore size distribution rather than just simply overall micropore volume. This important effect of the micropore size distribution on the methane adsorption isotherms will be used later to obtain information about the porous texture of the samples. Sample KUA1B8 was prepared with a view to gas separation, specifically CO_2 and CH_4. In this regard it was successful where short nonequilibrium exposure times are used. However, methane was adsorbed by this carbon when a much longer time exposure was allowed. Figure 2 presents this isotherm which shows that methane can penetrate into these narrow pores. Adsorption reached its saturation maximum by a pressure of 1 MPa indicating a very narrow pore structure and giving a micropore volume somewhat higher than that determined from low- or high-pressure 273 K CO_2, Tables 1 and 2.

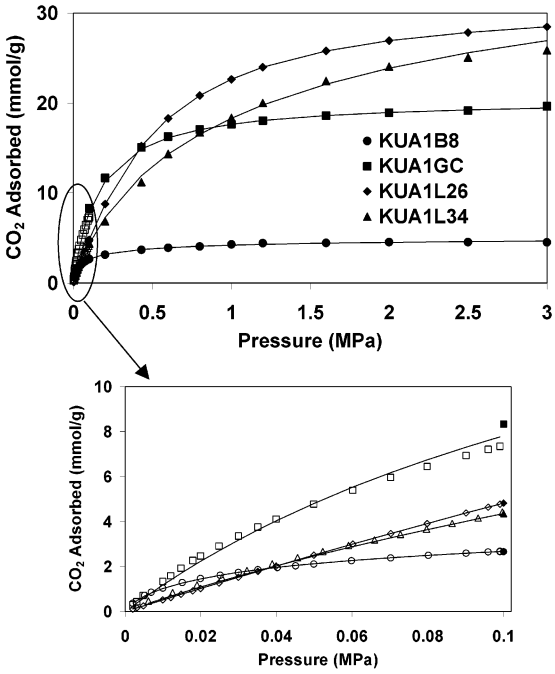

Figure 3. CO_2 adsorption isotherms at 273 K for the samples used in the present study. Points: experimental isotherms; lines: curve fittings obtained by applying the Toth equation.

Figure 3 presents the experimental CO_2 adsorption isotherms obtained at 273 K for the samples used in the present study (points) and the associated curve fittings obtained by applying the Toth equation lines. It should be mentioned that the carbon molecular sieve (KUA1B8) which could not be characterized by N_2 adsorption and it took very long time for the CH_4 adsorption, does present adsorption of CO_2 at 273 K, and its isotherms can be easily measured. Each isotherm depicts results obtained from the experiment performed at subatmospheric pressures, which covers a range of pressure from 2×10^{-3} MPa to 0.1 MPa (open points), and the isotherm done at high pressure, up to 3 MPa, in the gravimetric system (full points). In the zoom-in plot showed in Figure 3, it can be observed that there is a good continuation in the measurements done at subatmospheric and high pressures despite the different experimental systems used (volumetric for the low-pressure adsorption and gravimetric for the high-pressure adsorption). In Figure 3 it is also shown that the curve fittings obtained by applying the Toth equation are very good, although in the case of the sample with the widest MPSD (KUA1L34) there is a slight deviation at high pressure. Apart from that sample, it is seen that in the other cases the experimental isotherm is well represented by

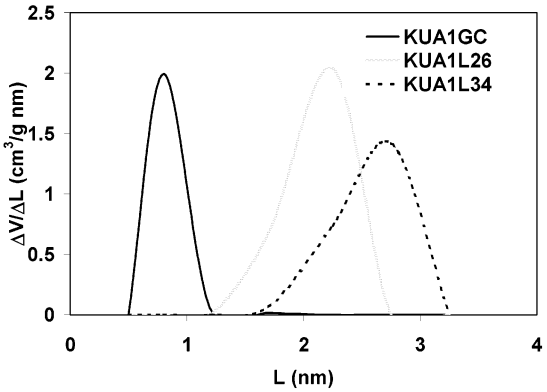

Figure 4. MPSDs obtained from the N_2 adsorption data using the approach proposed by Cazorla-Amorós et al.

the curve fitting including even the very closed knee corresponding to the sample (KUA1B8).

As in the case of N_2 and CH_4, the shape of the CO_2 adsorption isotherms carried out up to 3 MPa provides information about the porosity of the samples. All the CO_2 adsorption isotherms are of type I, characteristic of microporous materials. The samples KUA1B8 and KUA1GC present a sharper knee, reaching the isotherm plateau at around 1 MPa. This suggests that these samples present a narrower MPSD than the samples KUA1L26 and KUA1L34, which exhibit a much rounder knee.

The sample KUA1B8 has a much lower CO_2 adsorption capacity than the sample KUA1GC. This is expected since the former has been prepared by partially blocking the microporosity existing in an activated carbon with a porous texture very similar to the sample KUA1GC. After such a process, a sample with a much narrower MPSD is obtained, but also with a much lower micropore volume.

It should be remarked that the differences in the shape of the CO_2 isotherms for the samples studied are more clearly shown than in the case of N_2 adsorption isotherms. As pointed out by Cazorla-Amoros et al.,[24] this is due to CO_2 at 273 K filling micropores over a wider range of relative fugacities than N_2 adsorption at 77 K.

4.3. Assessment of Microporosity and Pore Size Distribution from N_2, CO_2, and CH_4 Adsorption Data. MPSDs have been calculated from both the high-pressure methane and CO_2 isotherms using the approaches described previously.[24,26] The pore size used in the MPSDs for each calculated interval is the mean pore size value of each interval range. These distributions cover five pore size ranges (from 0.38 to 3 nm). The larger pore ranges have been omitted since they did not show any significant pore volume. The pore sizes obtained by these approaches are the size available for the gases, i.e., the additional width of a carbon atom is not considered.

Figure 4 presents the MPSDs obtained from the N_2 adsorption data using the approach proposed in a previous work.[24] As expected from the characterization results at sub-atmospheric pressure (see Table 1), the narrowest MPSD corresponds to the sample KUA1GC (lowest difference between the micropore volume calculated from N_2 and CO_2 adsorption data; see Table 1). The other two samples clearly present wider MPSDs. To see the excellence of the fitting, Figure 5 shows the experimental isotherm (points) and the theoretical isotherms (line) calculated from the MPSDs.

In Figure 4 it can be seen that, essentially, the mean pore size values obtained from N_2 adsorption data do not correspond to the characteristics of the samples, specially in the case of the samples with wider pore size distribution, which are shifted

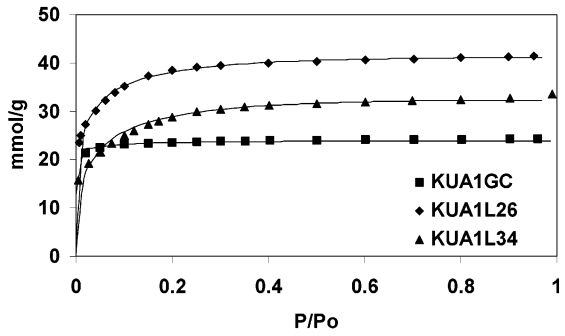

Figure 5. Experimental N_2 adsorption isotherms (points) and theoretical isotherms (line) calculated from the MPSDs.

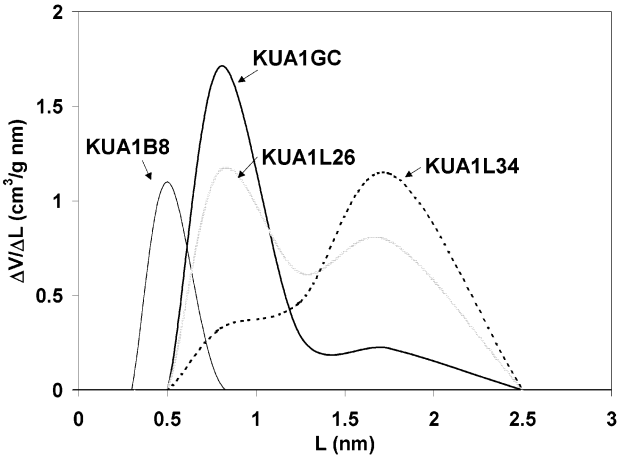

Figure 6. MPSDs for the four activated carbons obtained from the high-pressure methane adsorption isotherms.

up to the mesopore region. This could be due to both the lack of experimental points in the very low relative pressure range (limitations of the equipment used in the experiments of this paper) and to the approach used for calculating the MPSDs.

Figure 6 illustrates the MPSDs for the four activated carbons obtained using their high-pressure methane adsorption isotherm. It seems that the characterization of these types of samples using this approach, produces bimodal distributions, where the importance of each peak depends on the shape of the isotherm. According to these results from methane adsorption data, the samples with the narrowest MPSDs are the samples KUA1B8 and KUA1GC, presenting the maximum of the distributions at around 0.5 and 0.8 nm, respectively. The contribution of the second peak is important in the case of the sample with a higher activation degree (KUA1L26) and becomes very important in the case of the sample with the widest MPSD (sample KUA1L34).

Since all these carbons were prepared from the same raw material using the same activation process, they all show the same characteristic pore widths. The exception is sample KUA1B8 where the pores were deliberately blocked using an additional procedure. The least activated carbon, KUA1GC, presents its greatest pore volume in the 0.8 nm range with little in the 1.5−1.8 nm range. With increased activation, KUA1L26, shows a reduced pore volume in the 0.8 nm range while the volume of pores in the 1.5−1.8 nm range increases. Sample KUA1L34, which has been activated to the greatest extent, illustrates how this activation has greatly reduced the narrower pore size range volume and considerably increased the volume of the 1.5−1.8 nm pores. This gradual change with activation is not perceived from the PSDs obtained from nitrogen.

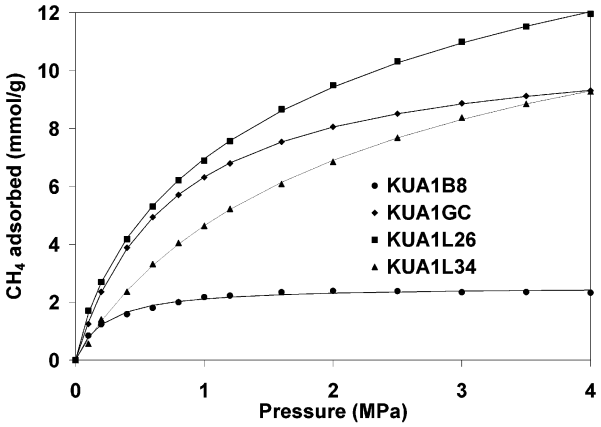

Figure 7. Methane isotherms constructed using the MPSDs and the methane density in each given pore at a particular pressure (lines). Experimental data points for the supercritical methane MPSDs.

Using the MPSDs and the methane density in each given pore at a particular pressure, the methane isotherms for the four activated carbons were constructed. Figure 7 shows these constructed isotherms from the supercritical methane MPSDs along with the experimental data points. The close agreement suggests that the use of the Toth equation for curve fitting of the isotherm is valid for all the pressure range.

On the other hand, the MPSDs obtained from the CO_2 adsorption data (sub-atmospheric and high-pressure adsorption data) for the four samples used in the present study are presented in Figure 8. These MPSDs show that the approach used in the analysis is consistent with the characteristics of the samples. As expected, the narrowest MPSDs corresponds to the carbon molecular sieve (sample KUA1B8). This sample presents a very homogeneous MPSD with most of the porosity having a pore size of 0.5 nm. As mentioned before, this sample has shown good separation capabilities for CH_4 and CO_2. Then, the mean pore size should be between 0.3 and 0.4 nm, which suggests that, in the case of this sample with very narrow pores, the obtained MPSD is slightly shifted to higher pore sizes. This could be due to the fact that the equation relating the mean width (L) and the characteristic energy (E_o) is an empirical equation and, probably, is not very precise for samples with very narrow pore sizes. The sample KUA1GC has also a quite narrow MPSD, although it presents some micropore volume at higher micropore size. This sample presents the maximum at around 0.8 nm, which completely agrees with the results obtained with the methane distributions.

As commented earlier, the sample KUA1B8 was prepared as a result of a pore blocking process using a sample with a very similar porous texture to the KUA1GC sample. In Figures 6 and 8 it can be observed that the effect of that pore blocking process is clearly reflected in the MPSDs, showing a drastic reduction of the total pore volume. With this treatment pores greater than approximately 0.8 nm disappear and the presence of very narrow micropores (pore size smaller than 0.5 nm) is detected. The fact that we can observe clearly the difference between these two samples indicates that the approach used for the analysis of high-pressure methane and CO_2 adsorption data is successful in presenting the characteristics of these samples, even though they have micropores with a very narrow size.

Figure 9 contains the fitting of the experimental CO_2 adsorption data using the procedure described above for the calculation of MPSDs from CO_2 adsorption data. It can be observed that the fitting obtained, using a maximum pore size of 3 nm, is quite good for all the samples.

Figures 4, 6, and 8 clearly show the changes of the width, and the shift of the maxima of the MPSDs for the series of samples studied in the present work. In the case of the sample KUA1GC, the mean pore size obtained with the three adsorptives is very similar. However, for the rest of the samples, the N_2 MPSDs gives higher mean pore width values than CH_4 and CO_2. As it has been previously commented, this could be a consequence of the lack of experimental data points in the relatively low pressure range. In the case of the CO_2 and CH_4, due to the experimental conditions, it is easy to obtain experimental points in the low relative pressure range. Thus, the experimentally difficult problem existing with N_2 is avoided, giving MPSDs with a mean pore size in the micropore range. This indicates that CO_2 and CH_4 are suitable for analyzing more sensibly the changes in the MPSD.

To more easily compare the MPSDs obtained with these two different adsorptives (CH_4 and CO_2) both at high pressure, Figure 10 presents in the same graphic both MPSDs for each of the four samples, which have been characterized with both adsorptives.

It is known that for the same adsorption data, different theoretical methods lead to different conclusions. Then, it should be expected that even more variation is likely to occur when using different adsorptives (CH_4 and CO_2) and different experimental temperatures (298 and 273 K, respectively), which

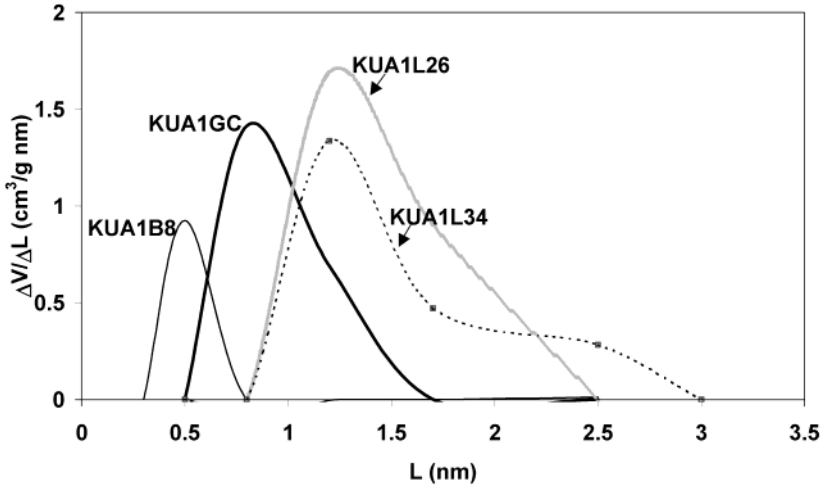

Figure 8. MPSDs obtained from the CO_2 adsorption data (sub-atmospheric and high-pressure adsorption data) for the four samples used in the present study.

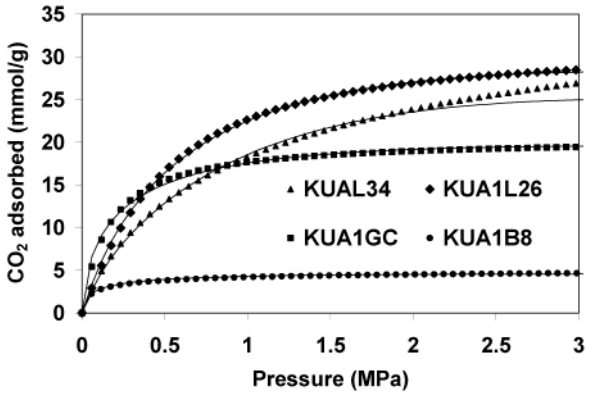

Figure 9. Fitting of the experimental CO_2 adsorption data using the procedure for the calculation of MPSDs from CO_2 adsorption data.

correspond to different adsorption conditions (supercritical in the case of CH_4 and subcritical in the case of CO_2). However, as can be observed in Figure 10, a reasonable consistency between both MPSDs exists for all the cases.

From the calculations used for high-pressure methane and CO_2 MPSDs, it is easy to obtain the micropore volume (by summing the pore volume of each range pore size below 2 nm). Table 2 contains the micropore volumes obtained from the high-pressure methane and CO_2 isotherms (V_{CH_4} and V_{CO_2}HP, respectively). If the micropore calculated from the MPSD obtained from low and high-pressure adsorption data (Table 2) are compared with those calculated from subatmospheric adsorption data (Table 1), it can be seen that in the case of the sample KUA1B8, both values are almost the same ($V_{CO_2} \approx V_{CO_2}$HP) while V_{CH_4} is somewhat higher. Something similar happens with the sample with very narrow micropore size distribution (KUA1GC). However, in the case of the samples with a wide MPSD (KUA1L26 and KUA1L34) the micropore volumes calculated from high-pressure CO_2 adsorption data are higher than the values obtained from low pressure. This is expected because CO_2 adsorption at subatmospheric pressure only considers the narrow micropore, while CO_2 adsorption at high pressure accounts for the whole microporosity.[23−25] The micropore volume obtained from adsorption at high pressure (CO_2 and CH_4) are quite close. This fact reflects, again, the consistency of both approaches, even though they use different adsorptives at different temperatures.

5. Conclusions

The shape of the experimental N_2, CO_2, and CH_4 high-pressure adsorption isotherms are very different between a series of microporous carbon materials prepared for the use in gas separation and methane storage. These differences are due in part to differences in the overall micropore volume, but additionally and importantly are due to the significant differences in the micropore size distribution of those samples.

Micropore size distributions (MPSDs) have been deduced from those N_2, CO_2, and CH_4 isotherms by application of the GAI, according to two different approaches proposed in previous independent works. In the case of N_2, the mean pore size values for the samples with wide MPSDs are shifted to the mesopore range. In contrast, the results obtained in the CO_2 and CH_4 analysis are very consistent with the characteristics of the samples suggesting that both methods are suitable to analyze more sensibly the changes in the MPSDs of microporous samples. There are mainly two reasons which make the use of CO_2 and CH_4 more directly related to the characterization of activated carbons prepared for natural gas storage and gas separation, rather than MPSDs obtained by using another gas at much lower pressures and temperature, as, for example, nitrogen adsorption at 77 K. These two reasons are (i) these MPSDs analysis are based on high-pressure adsorption isotherms, and (ii) the CO_2 is especially useful to characterize the narrow microporosity not accessible to N_2 and very difficult

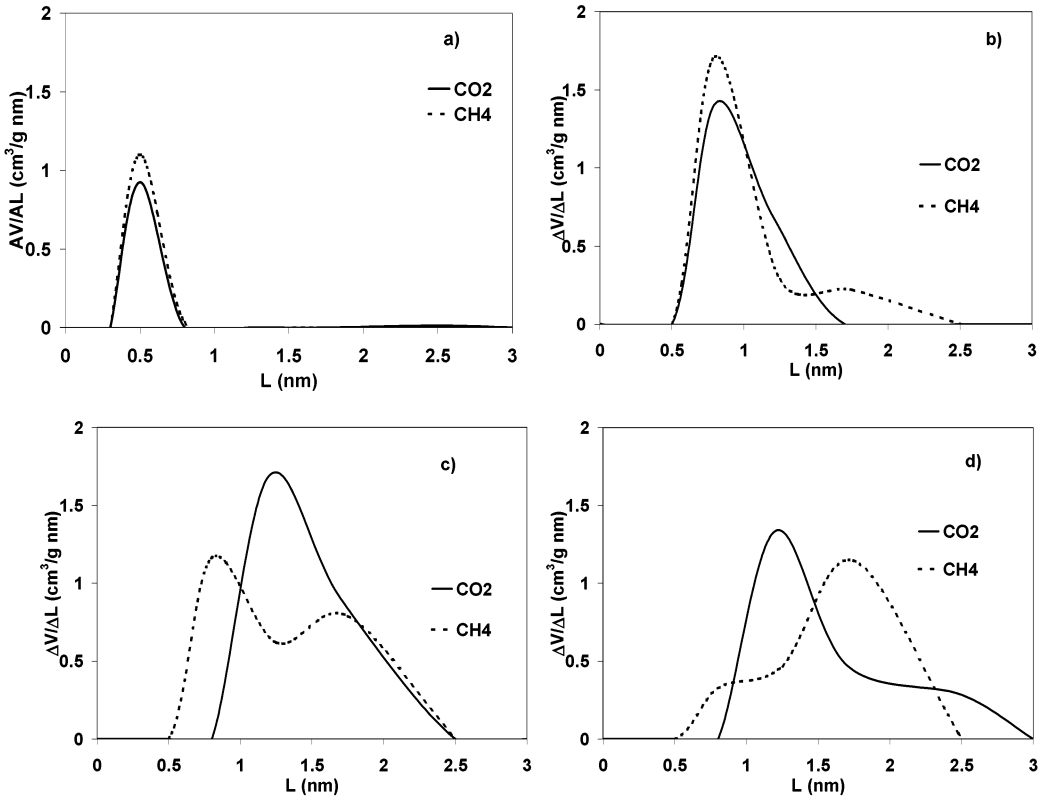

Figure 10. Comparison of MPSDs obtained from CO_2 and CH_4 adsorption data for each of the four samples.

for CH_4 to access. In addition, for applications such as natural gas storage where changes in pore structure are important, analysis of the methane isotherms presents a bimodal PSD for these carbons while nitrogen suggests only a unimodal structure. This may not be inherently due to the different gases but results from the alternative methods in the determination of the PSDs.

The comparison of the results from both adsorptives has shown that, despite the different characteristics of CH_4 and CO_2, and the different experimental temperatures and adsorption conditions (298 K, supercritical conditions, and 273 K, subcritical conditions, respectively), a quite good consistency between the MPSDs from these two gases has been obtained for all the samples studied.

Acknowledgment. The authors thank MCYT (Projects MAT 2000-0621) for financial support. D. Lozano-Castelló thanks MEC for the thesis grant.

References and Notes

(1) Parkyns, N. D.; Quinn, D. F. *Porosity in Carbons*; Patrick, J. W., Ed.; Edward Arnold: 1995; p 293.
(2) Menon, V. C.; Komarneni, S. *J. Porous Mater.* **1998**, *5*, 43.
(3) Cook, T. L.; Komodromos, C.; Quinn, D. F.; Ragan, S.*Carbon Materials for Advanced Technologies*; Burchell, T. D., Ed.; Elsevier Science: New York, 1999; p 269.
(4) Alcaniz-Monge, J.; De la Casa-Lillo, M. A.; Cazorla-Amorós, D.; Linares-Solano, A. *Carbon* **1997**, *35*, 291.
(5) De la Casa-Lillo, M. A.; Alcaniz-Monge, J.; Raymundo-Pinero, E.; Cazorla-Amorós, D.; Linares-Solano, A. *Carbon* **1998**, *36*, 1353.
(6) Lozano-Castelló, D.; Lillo-Ródenas, M. A.; Cazorla-Amorós, D.; Linares-Solano, A. *Carbon* **2001**, *39*, 741.
(7) Lozano-Castelló, D.; De la Casa-Lillo, M. A.; Cazorla-Amorós, D.; Linares-Solano, A. *Carbon Conference* **1999**; p 626.
(8) Alcaniz-Monge, J.; Lozano-Castelló, D.; Cazorla-Amorós, D.; Linares-Solano, A. *Carbon Conference* **1999**; p 682.
(9) Lozano-Castelló, D.; Cazorla-Amorós, D.; Linares-Solano, A.; Quinn, D. F. *Carbon*, in press.
(10) Matranga, K. R.; Myers, A. L.; Glandt, E. D. *Chem. Eng. Sci.* **1992**, *47*, 1569.
(11) Aukett, P. N.; Quirke, N.; Riddiford, S.; Tennison, S. R. *Carbon* **1992**, *30*, 913.
(12) Cracknell, R. F.; Gordon, P.; Gubbins, K. E. *J. Phys. Chem.* **1993**, *97*, 494.
(13) Chen, X. S.; McEnaney, B.; Mays, T. J.; Alcañiz-Monge, J.; Cazorla-Amorós, D.; Linares-Solano, A. *Carbon* **1997**, *35*, 1251.
(14) Lozano-Castelló, D.; Cazorla-Amorós, D.; Linares-Solano, A.; Hall, P. J.; Gascon, D.; Galan, C. *Carbon* **2001**, *39*, 1343.
(15) Verma, S. K.; Walker, P. L., Jr. *Carbon* **1992**, *30*, 837.
(16) Rouquerol, J.; Avnir, D.; Everett, D. H.; Fairbridge, C.; Hoynes, M.; Pernicone, N.; Ramsay, J. D. F.; Sing, K. S. W. *Characterisation of Porous Solids;* Unger, K. K. et al., Eds.; 1994; 1.
(17) Stoeckli, F. *Carbon* **1989**, *27*, 962.
(18) Jaroniec, M.; Choma, J. *Carbon* **1988**, *26*, 747.
(19) Horvath, G.; Kawazoe, J. *J. Chem. Eng. Jpn*. **1983**, *16*, 470.
(20) Mays, T. J. *Fundamental of adsorption*; Le Van, M. D., Ed.; Kluwer: Dordrecht, The Netherlands, 1996; p 603.
(21) Seaton, N. A.; Walton, J. P. R. B.; Quirke, N. A. Carbon **1989**, *27*, 853.
(22) Rodríguez-Reinoso, F.; Linares-Solano, A. *Chem. Phys. Carbon* **1988**, *21*, 1.
(23) Cazorla-Amorós, D.; Alcañiz-Monge, J.; Linares-Solano, A. *Langmuir* **1996**, *12*, 2820.
(24) Cazorla-Amorós, D.; Alcañiz-Monge, J.; De la Casa-Lillo, M. A.; Linares-Solano, A. *Langmuir* **1998**, *14*, 4589.
(25) Linares-Solano, A.; Salinas-Martínez de Lecea, C.; Alcañiz-Monge, J.; Cazorla-Amorós, D. *Tanso* **1998**, *185*, 316.
(26) Sosin, K. A.; Quinn, D. F. *J. Porous Mater.* **1995**, *1*, 111.
(27) Sosin, K. A.; Quinn, D. F.; MacDonald, J. A. F. *Carbon* **1996**, *34*, 1335.
(28) Lozano-Castelló, D.; Cazorla-Amorós, D.; Linares-Solano, A.; Quinn, D. F. *Carbon Conference* **2000**, p 131.
(29) Gusev, V. Y.; O'brien, J. A.; Seaton, N. A. *Langmuir* **1997**, *13*, 2815.
(30) Zhou, L.; Zhou, Y.; Ming, L.; Chen, P.; Wang, Y. *Langmuir* **2000**, *16*, 5955.
(31) Nguyen, C.; Do, D. D. *J. Phys. Chem. B* **1999**, *103*, 6900.
(32) Nguyen, C.; Do, D. D. *Langmuir* **2000**, *16*, 1319.
(33) Sun, J.; Chen, S.; Rood, M. J.; Rostam-Abadi, M. *Energy Fuels* **1998**, *12*, 1071.
(34) Zhou, L.; Ming, L.; Zhou, Y. *Sci. China, Ser. B* **2000**, *43*, 145.
(35) Scaife, S.; Kluson, P.; Quirke, N. *J. Phys. Chem. B* **2000**, *104*, 313.
(36) Sweatman, M. B.; Quirke, N. *J. Phys. Chem. B* **2001**, *105*, 1403.
(37) Samios, S.; Stubos, A. K.; Kanellopoulos, N. K.; Cracknell, R. F.; Papadopoulos, G. K.; Nicholson, D. *Langmuir* **1997**, *13*, 2795.
(38) Vishnyakov, A.; Ravikovitch, I.; Neimark, A. V. *Langmuir* **1999**, *15*, 8736.
(39) Samios, S.; Stubos, A. K.; Papadopoulos, G. K.; Kanellopoulos, N. K.; Rigas, F. *J. Colloid Interface Sci.* **2000**, *224*, 272.
(40) Ravikovitch, P. I.; Vishnyakov, A.; Russo, R.; Neimark, A. V. *Langmuir* **2000**, *16*, 2311.
(41) Stoeckli, F.; Guillot, A.; Slasli, A. M.; Hugi-Cleary, D. *Carbon* **2002**, *40*, 383−388.
(42) McEnaney, B.; Mays, T. J.; Causton, P. D. *Langmuir* **1987**, *3*, 695.
(43) Tan, Z.; Gubbins, E. *J. Phys. Chem.* **1992**, *94*, 6061.
(44) Dubinin, M. M. *Chem. Rev.* **1960**, *60*, 235.
(45) Hutson, N. D.; Yang, R. T. *Adsorption* **1997**, *3*, 189.
(46) Stoeckli, F.; Ballerini, L. *Fuel* **1991**, *70*, 557.
(47) Dubinin, M. M. Carbon **1985**, *23*, 373.
(48) Agarwal, R. K.; Schwarz, J. A. *Carbon* **1988**, *26*, 873.
(49) DeGance, A. E. *Fluid Phase Equilib.* **1992**, *78*, 99.
(50) Sing, K. S. W.; Everett, D. H.; Haul, R. A. W.; Moscou, L.; Pierotti, R. A.; Rouquerol, J.; Siemieniewska, T. *Pure Appl. Chem.* **1985**, *57*, 603.
(51) Alcañiz-Monge, J.; Cazorla-Amorós, D.; Linares-Solano, A.; Yoshida, S.; Oya, A. *Carbon* **1994**, *32*, 1277.
(52) Breck, D. W. *Zeolite Molecular Sieves. Structure, chemistry, and use;* Krieger RE Publishing Company: Florida, 1974.
(53) Toth, J. *Fundamentals of Adsorption*; Myers, A. L., Belfort, G., Eds.; 1984; p 657.